A direct method for cyclic crystal plasticity with application to high-cycle fatigue

Insaf Echerradi, Daniel Weisz-Patrault, Michaël Peigney

A direct method for cyclic crystal plasticity with application to high-cycle fatigue

Insaf Echerradi[1], Daniel Weisz-Patrault[2], Michael Peigney[1]

[1] Lab Navier, Univ Gustave Eiffel, ENPC, CNRS, F-77447 Marne la Vallée, France
[2] LMS, CNRS, École Polytechnique, Institut Polytechnique de Paris, F-91128 Palaiseau, France

Abstract. The prediction of fatigue in materials and structures is usually based on experimental Wohler curves, relating the number of cycles to failure to the amplitude of the applied cyclic loading. Those curves show some scattering due notably to the variability of the microstructure. Predicting fatigue lifetime can thus be seen as a statistical problem that depends on microstructural descriptors. This paper paves the way to a probabilistic approach for quantitatively linking crystallographic and morphological texture data to fatigue lifetime prediction. In more detail, a simplified mesoscopic model is constructed for calculating the evolution of an elastic-plastic polycrystal with a prescribed texture. That model is limited to high cycle fatigue, corresponding to cyclic loadings of sufficiently low amplitude for plasticity to be mainly confined to few well-separated grains. The model obtained takes details of the texture into account, i.e. the distribution, shape and orientation of the individual grains. It relies on analytical formula and is mesh-free. A comparison with full-field finite element simulation shows that the proposed model leads to satisfactory results in regard to its complexity. In the case of cyclic loading, we show that the model presented leads to a direct method for calculating the asymptotic values of the plastic slips (and cumulated plastic slips) reached in each grain when the number of cycles grows to infinity. We show how that direct approach can be used for upscaling a local failure criterion to the mesoscopic scale and performing probabilistic analysis.

Keywords: High cycle fatigue · Mesoscopic model · Crystal plasticity· Incremental energy minimization · Direct method.

1 Introduction

It is commonly accepted that fatigue in polycrystals is related to plastic mechanisms occurring at the grain scale. Plastic flow initiates in few critical grains having the least favorable orientations with respect to the applied loading. For small loading amplitudes, plasticity remains confined in those grains but persistent slip bands may appear after a large number of cycles, leading to the possible initiation of a crack. Based on that interpretation, the fatigue life of a polycrystal

could in principle be predicted from the elastic-plastic evolution of its constitutive grains. Some work in that direction can notably be found in [1] using full-field simulations. For such problems, direct methods bypassing the incremental simulation over a large number of cycles are of interest. A possible approach is to use shakedown theory. In classical plasticity, Melan and Koiter theorems deliver bounds on the set of loadings for which there is elastic shakedown, i.e. the plastic dissipation is bounded on the time interval $[0, +\infty)$. In more intuitive terms, shakedown means that the medium behaves elastically in the large time limit. Those theorems have been extended to several types of nonlinear behaviors [17–19, 24, 8, 20, 21] and can be used to bound the shakedown domain of a polycrystal with a given microstructure. Since shakedown is beneficial for fatigue, loadings within the shakedown domain are expected to correspond to high-cycle fatigue. A recent illustration of that approach can be found in [15]. However, although shakedown is a requisite for high-cycle fatigue, it does not guarantee an infinite lifetime. Indeed, the number of cycles to failure depends on the asymptotic state of stress reached in the polycrystal, which shakedown theory only provides limited information about. Sects 2–4 of this paper report on a simplified numerical method for a fast evaluation of the plastic slips in elastic-plastic 2D polycrystals. That method is based on incremental variational principles, which have proved to be a fruitful approach in many applications [9, 10, 2, 16, 26, 22, 25]. Starting from elastic-plastic constitutive equations detailed in Sect. 2, the incremental evolution problem is turned into an energy minimization problem over the space of admissible displacement fields and plastic slip fields (Sect. 3). An approximate solution can be obtained by restricting the minimization to a well-chosen finite dimensional subspace, in the spirit of Galerkin's methods. In the present case, we restrict the energy minimization to plastic strain fields that are uniform per grain. For an isotropic elasticity tensor, the incremental problem reduces to a linear complementarity problem. That problem can further be simplified by neglecting the elastic interaction between plastifying grains and assuming that only one plastic slip system is activated in each grain. Such assumptions are expected to be representative of small loadings corresponding to high-cycle fatigue. In that case, the incremental problem can be solved analytically as detailed in Sect. 4. The increment of plastic slip in grain j is obtained as an explicit function of the material parameters, loading parameters and a localization tensor $\boldsymbol{S}^j$ that is entirely determined from the geometry of the grain and the elastic moduli. For an ellipsoidal grain, the tensor $\boldsymbol{S}^j$ corresponds to the Eshelby tensor [5, 14]. The validity of the model presented is briefly discussed in Sect. 5 by comparison with full-field finite element simulations. The approach presented allows one to estimate the step-by-step evolution of plastic slips for a given loading history. In Sect. 6 we focus on cyclic loadings and show that the approach presented leads to a direct method for calculating the asymptotic values taken by the state variables in each grain as the number of cycles grows to infinity. That method is direct in the sense that it gives the asymptotic state without resorting to step-by-step calculation. The direct approach of Sect. 6 is used in Sect. 7 for upscaling a local (microscopic) fatigue criterion to the mesoscopic scale of a polycrystal: starting

from a crack initiation criterion at the grain level, we use the asymptotic formulas of the shakedown state to express the fatigue criterion at the mesoscopic level. The mathematical structure of the obtained fatigue criterion is compared with well-established fatigue criteria (Dang Van, Crossland, Sines). In Sect. 8 we show how the model presented can be used in a probabilistic setting.

2 Constitutive laws

2.1 Single crystal

First consider a single crystal modeled in the framework of crystalline plasticity at small strains: considering N slip systems $(\boldsymbol{n}_i, \boldsymbol{t}_i)_{1\leq i\leq N}$, the local strain $\boldsymbol{\varepsilon}$ is decomposed as

$$\boldsymbol{\varepsilon} = \boldsymbol{C}^{-1} : \boldsymbol{\sigma} + \sum_{i=1}^{N} \gamma_i \boldsymbol{\tau}_i^0 \tag{1}$$

where

$$\boldsymbol{\tau}_i^0 = \frac{1}{2}(\boldsymbol{n}_i \otimes \boldsymbol{t}_i + \boldsymbol{t}_i \otimes \boldsymbol{n}_i) \tag{2}$$

and $(\gamma_i, \boldsymbol{n}_i, \boldsymbol{t}_i)$ are respectively the plastic slip, the normal to the slip plane and the slip direction for slip system i. In (1), $\boldsymbol{\sigma}$ is the stress and $\boldsymbol{C}$ is the elasticity tensor (assumed to be isotropic in the following). We recall that the strain $\boldsymbol{\varepsilon}$ is related to the displacement $\boldsymbol{u}$ by the relation $\boldsymbol{\varepsilon} = (\nabla \boldsymbol{u} + \nabla^T \boldsymbol{u})/2$. Adopting the framework of generalized standard materials [6], the plasticity flow rule is determined from the free energy Ψ and the dissipation potential Φ, which are respectively chosen as

$$\Psi = \frac{1}{2}(\boldsymbol{\varepsilon} - \sum_{i=1}^{N} \gamma_i \boldsymbol{\tau}_i^0) : \boldsymbol{C} : (\boldsymbol{\varepsilon} - \sum_{i=1}^{N} \gamma_i \boldsymbol{\tau}_i^0) + \frac{1}{2}\xi_X \sum_{i=1}^{N} \gamma_i^2 \tag{3}$$

$$\Phi = \sum_{i=1}^{N} (\tau_c + \xi \eta_i) |\dot{\gamma}_i| \tag{4}$$

where

$$\eta_i = \int_0^t |\dot{\gamma}_i| dt$$

is the accumulated plastic slip, $\tau_c > 0$ is the critical shear stress, $\xi_X \geq 0$ is the linear hardening modulus and $\xi \geq 0$ is the isotropic hardening modulus. The flow rule reads as

$$\boldsymbol{\sigma} : \boldsymbol{\tau}_i^0 - \xi_X \gamma_i \begin{cases} = \tau_c + \xi \eta_i & \text{if } \dot{\gamma}_i > 0 \\ = -\tau_c - \xi \eta_i & \text{if } \dot{\gamma}_i < 0 \\ \in [-\tau_c - \xi \eta_i, \tau_c + \xi \eta_i] & \text{if } \dot{\gamma}_i = 0 \end{cases} \tag{5}$$

2.2 Polycrystal

Now consider a polycrystalline Representative Volume Element (RVE) constituted of M grains occupying the disjoint subdomains $\Omega^1, \cdots, \Omega^M$. The crystalline orientation in grain j is characterized by a rotation $\boldsymbol{R}^j$ relative to the reference crystal, so that the constitutive equations in grain j are obtained by replacing $\boldsymbol{\tau}_i^0$ with $\boldsymbol{\tau}_i^j = {}^T\boldsymbol{R}^j\boldsymbol{\tau}_i^0\boldsymbol{R}^j$ in (1) and (5), i.e. for $\boldsymbol{x} \in \Omega^j$ we have the relations

$$\boldsymbol{\varepsilon} = \boldsymbol{C}^{-1} : \boldsymbol{\sigma} + \sum_{i=1}^{N} \gamma_i \boldsymbol{\tau}_i^j \tag{6}$$

$$\boldsymbol{\sigma} : \boldsymbol{\tau}_i^j - \xi_X \gamma_i \begin{cases} = \tau_c + \xi\eta_i & \text{if } \dot{\gamma}_i > 0, \\ = -\tau_c - \xi\eta_i & \text{if } \dot{\gamma}_i < 0, \\ \in [-\tau_c - \xi\eta_i, \tau_c + \xi\eta_i] & \text{if } \dot{\gamma}_i = 0. \end{cases} \tag{7}$$

We note than in the more general situation where the elasticity tensor $\boldsymbol{C}$ is not isotropic, the term $\boldsymbol{C}$ in (6) should be replaced with a rotated elasticity tensor depending on $\boldsymbol{R}^j$. The RVE is submitted to traction force $\bar{\boldsymbol{\sigma}}(t) \cdot \boldsymbol{n}$ on its boundary, where $\bar{\boldsymbol{\sigma}}(t)$ can be interpreted as the mesoscopic stress at time t. We consider a proportional loading of the form

$$\bar{\boldsymbol{\sigma}}(t) = f(t)\boldsymbol{\sigma}_0 \tag{8}$$

where $\boldsymbol{\sigma}_0$ is independent of time. Assuming quasistatic evolutions, the stress field needs to satisfy the equilibrium equations

$$\operatorname{div} \boldsymbol{\sigma} = 0 \text{ in } \Omega,\ \boldsymbol{\sigma} \cdot \boldsymbol{n} = \bar{\boldsymbol{\sigma}} \cdot \boldsymbol{n} \text{ on } \partial\Omega \tag{9}$$

where $\Omega = \cup_{j=1}^{M} \Omega^j$ is the domain occupied by the RVE. To simplify the presentation, the same critical shear stress τ_c and hardening moduli are used for all the grains.

3 Incremental energy minimization

For solving the evolution problem defined by Eqs (6), (7) and (9), a common approach is to resort to time-discretization: the evolution is calculated in a time marching approach, using an incremental problem for estimating the state variable $(\boldsymbol{\varepsilon}, \boldsymbol{\sigma}, \gamma_i, \eta_i)$ at time $t^0 + \delta t$ $(\delta t > 0)$, assuming their values $(\boldsymbol{\varepsilon}^0, \boldsymbol{\sigma}^0, \gamma_i^0, \eta_i^0)$ to be known. Adopting the backward Euler scheme, the corresponding incremental problem reads as

$$\begin{aligned} &\operatorname{div} \boldsymbol{\sigma} = 0 \text{ in } \Omega,\ \boldsymbol{\sigma} \cdot \boldsymbol{n} = \bar{\boldsymbol{\sigma}} \cdot \boldsymbol{n} \text{ on } \partial\Omega \\ &\boldsymbol{\varepsilon} = \boldsymbol{C}^{-1} : \boldsymbol{\sigma} + \sum_{i=1}^{N} \gamma_i \boldsymbol{\tau}_i^j \text{ in } \Omega^j \\ &\boldsymbol{\sigma} : \boldsymbol{\tau}_i^j - \xi_X \gamma_i \begin{cases} = \tau_c + \xi\eta_i & \text{if } \gamma_i > \gamma_i^0 \\ = -\tau_c - \xi\eta_i & \text{if } \gamma_i < \gamma_i^0 \\ \in [-\tau_c - \xi\eta_i \tau_c + \xi\eta_i] & \text{if } \gamma_i = \gamma_i^0 \end{cases} \text{ in } \Omega^j, \end{aligned} \tag{10}$$

with $\eta_i = \eta_i^0 + |\gamma_i - \gamma_i^0|$. A variational formulation is attached to the incremental problem (10). Setting $\boldsymbol{\gamma} = (\gamma_1, \cdots, \gamma_N)$, it can be verified indeed that the displacement field $\boldsymbol{u}$ and plastic slips field $\boldsymbol{\gamma}$ in (10) are solution to the minimization problem

$$\inf_{\boldsymbol{u},\boldsymbol{\gamma}} F \tag{11}$$

where

$$F = \sum_{j=1}^{M} \int_{\Omega^j} \Psi^j d\Omega + \sum_{i=1}^{N} \int_{\Omega} (\tau_c + \xi\eta_i^0 + \frac{1}{2}\xi\ |\gamma_i - \gamma_i^0|)|\gamma_i - \gamma_i^0| d\Omega - \int_{\partial\Omega} (\bar{\boldsymbol{\sigma}} \cdot \boldsymbol{n}) \cdot \boldsymbol{u} dS$$

and Ψ^j is the free energy in grain j, defined by replacing $\boldsymbol{\tau}_j^0$ with $\boldsymbol{\tau}_j^i$ in (3). Observing that $\int_{\partial\Omega} (\bar{\boldsymbol{\sigma}}.\boldsymbol{n}).\boldsymbol{u} \mathrm{d}S = \int_{\Omega} \bar{\boldsymbol{\sigma}} : \boldsymbol{\varepsilon} d\Omega$, we can rewrite F as

$$\begin{aligned} F = &\sum_{j=1}^{M} \int_{\Omega^j} \frac{1}{2}(\boldsymbol{\varepsilon} - \sum_{i=1}^{N} \gamma_i \boldsymbol{\tau}_i^j) : \boldsymbol{C} : (\boldsymbol{\varepsilon} - \sum_{i=1}^{N} \gamma_i \boldsymbol{\tau}_i^j) d\Omega + \frac{1}{2}\xi_X \int_{\Omega} \sum_{i=1}^{N} \gamma_i^2 d\Omega \\ &+ \sum_{i=1}^{n} \int_{\Omega} (\tau_c + \xi\eta_i^0 + \frac{1}{2}\xi\ |\gamma_i - \gamma_i^0|)|\gamma_i - \gamma_i^0| d\Omega - \int_{\Omega} \bar{\boldsymbol{\sigma}} : \boldsymbol{\varepsilon} d\Omega \end{aligned}$$

In general, problem (10) or (11) needs to be solved numerically, using e.g. the finite element method. Following [23], we note that problem (11) is mathematically equivalent to a linear complementarity problem. Dedicated numerical algorithms are available for such problems [3]. In the following we introduce a series of simplifying assumptions that allow us to solve (10) in a semi-analytical form. Those assumptions are expected to be relevant for small loadings corresponding to the regime of high-cycle fatigue.

4 Simplified problem

4.1 Piecewise-constant plastic slips

We restrict the minimization in (11) to plastic slips that are uniform in each grain. That assumption notably allows one to make some progress on the minimization of (11) with respect to $\boldsymbol{u}$. For a given $\boldsymbol{\gamma}$ (uniform per grain), observe indeed that

$$\begin{aligned} \inf_{\boldsymbol{u}} F = &\frac{1}{2}\xi_X \int_{\Omega} \sum_{i=1}^{N} \gamma_i^2 d\Omega + \sum_{i=1}^{N} \int_{\Omega} (\tau_c + \xi\eta_i^0 + \frac{1}{2}\xi\ |\gamma_i - \gamma_i^0|)|\gamma_i - \gamma_i^0| d\Omega \\ &+ \frac{1}{2} \sum_{j=1}^{M} |\Omega^j| \boldsymbol{\tau}^j : \boldsymbol{C} : \boldsymbol{\tau}^j + W \end{aligned}$$

where

$$W = \inf_{\boldsymbol{u}} \frac{1}{2} \int_{\Omega} \boldsymbol{\varepsilon} : \boldsymbol{C} : \boldsymbol{\varepsilon} d\Omega - \sum_{j=1}^{M} \int_{\Omega^j} \boldsymbol{\varepsilon} : \boldsymbol{C} : \boldsymbol{\tau}^j d\Omega - \int_{\Omega} \bar{\boldsymbol{\sigma}} : \boldsymbol{\varepsilon} d\Omega \tag{12}$$

and $\boldsymbol{\tau}^j = \sum_{i=1}^{N} \gamma_i \boldsymbol{\tau}_i^j$. Let χ^j be the characteristic function of Ω^j, i.e. $\chi^j(\boldsymbol{x}) = 1$ if $\boldsymbol{x} \in \Omega^j$ and $\chi^j(\boldsymbol{x}) = 0$ otherwise. Setting $\boldsymbol{\tau}(\boldsymbol{x}) = \boldsymbol{C}^{-1} : \bar{\boldsymbol{\sigma}} + \sum_j \chi^j(\boldsymbol{x})\boldsymbol{\tau}^j$, we obtain

$$W = \inf_{\boldsymbol{u}} \frac{1}{2} \int_\Omega \boldsymbol{\varepsilon} : \boldsymbol{C} : \boldsymbol{\varepsilon} d\Omega - \int_\Omega \boldsymbol{\varepsilon} : \boldsymbol{C} : \boldsymbol{\tau} d\Omega. \tag{13}$$

The solution $\boldsymbol{u}^*$ to the minimization problem (13) satisfies the stationarity condition

$$\int_\Omega \boldsymbol{\varepsilon}^* : \boldsymbol{C} : \boldsymbol{\varepsilon} d\Omega = \int_\Omega \boldsymbol{\tau} : \boldsymbol{C} : \boldsymbol{\varepsilon} d\Omega \tag{14}$$

for any compatible strain field $\boldsymbol{\varepsilon}$. Using (14) with $\boldsymbol{\varepsilon} = \boldsymbol{\varepsilon}^*$ gives $\int_\Omega \boldsymbol{\varepsilon}^* : \boldsymbol{C} : \boldsymbol{\varepsilon}^* d\Omega = \int_\Omega \boldsymbol{\tau} : \boldsymbol{C} : \boldsymbol{\varepsilon}^* \mathrm{d}\Omega$ so that

$$W = -\frac{1}{2} \int_\Omega \boldsymbol{\tau} : \boldsymbol{C} : \boldsymbol{\varepsilon}^* d\Omega. \tag{15}$$

Choosing $\boldsymbol{\varepsilon} = \int_\Omega (\boldsymbol{\varepsilon}^* - \boldsymbol{\tau}) \mathrm{d}\Omega$ in (14) gives $\int_\Omega \boldsymbol{\varepsilon}^* d\Omega = \int_\Omega \boldsymbol{\tau} d\Omega = |\Omega| \boldsymbol{C}^{-1} : \bar{\boldsymbol{\sigma}} + \sum_j |\Omega^j| \boldsymbol{\tau}^j$ so that

$$\begin{aligned} \int_\Omega \boldsymbol{\tau} : \boldsymbol{C} : \boldsymbol{\varepsilon}^* d\Omega &= \bar{\boldsymbol{\sigma}} : \int_\Omega \boldsymbol{\varepsilon}^* d\Omega + \sum_j \boldsymbol{\tau}^j : \boldsymbol{C} : \left(\int_{\Omega^j} \boldsymbol{\varepsilon}^* d\Omega \right) \\ &= |\Omega| \bar{\boldsymbol{\sigma}} : \boldsymbol{C}^{-1} : \bar{\boldsymbol{\sigma}} + \sum_j |\Omega^j| \bar{\boldsymbol{\sigma}} : \boldsymbol{\tau}^j + \sum_j \boldsymbol{\tau}^j : \boldsymbol{C} : \left(\int_{\Omega^j} \boldsymbol{\varepsilon}^* d\Omega \right). \end{aligned} \tag{16}$$

Note that $\boldsymbol{u}^*$ is a solution to the linear elasticity problem

$$\begin{aligned} &\boldsymbol{\sigma}^* = \boldsymbol{C} : (\boldsymbol{\varepsilon}^* - \boldsymbol{\tau}^j) \text{ in } \Omega^j, \\ &\boldsymbol{\varepsilon}^* = (\nabla \boldsymbol{u}^* + \nabla^T \boldsymbol{u}^*)/2, \\ &\operatorname{div} \boldsymbol{\sigma}^* = 0 \text{ in } \Omega, \\ &\boldsymbol{\sigma}^* \cdot \boldsymbol{n} = \bar{\boldsymbol{\sigma}} \cdot \boldsymbol{n} \text{ on } \partial\Omega. \end{aligned} \tag{17}$$

The superposition principle implies that

$$\boldsymbol{\varepsilon}^* = \boldsymbol{C}^{-1} : \bar{\boldsymbol{\sigma}} + \sum_j \boldsymbol{\varepsilon}^j \tag{18}$$

where $\boldsymbol{\varepsilon}^j$ is the strain field corresponding to the solution of the *single inclusion problem* (defined for any given $j = 1, \cdots, M$)

$$\begin{aligned} &\boldsymbol{\sigma} = \boldsymbol{C} : (\boldsymbol{\varepsilon}^j - \boldsymbol{\tau}^j) \text{ in } \Omega^j, \\ &\boldsymbol{\sigma} = \boldsymbol{C} : \boldsymbol{\varepsilon}^j \text{ in } \Omega - \Omega^j, \\ &\boldsymbol{\varepsilon}^j = (\nabla \boldsymbol{u}^j + \nabla^T \boldsymbol{u}^j)/2, \\ &\operatorname{div} \boldsymbol{\sigma} = 0 \text{ in } \Omega, \\ &\boldsymbol{\sigma} \cdot \boldsymbol{n} = 0 \text{ on } \partial\Omega. \end{aligned} \tag{19}$$

Problem (19) is linear in $\boldsymbol{\tau}^j$ so that $\boldsymbol{\varepsilon}^j(\boldsymbol{x})$ can be written as

$$\boldsymbol{\varepsilon}^j(\boldsymbol{x}) = \boldsymbol{S}^j(\boldsymbol{x}) : \boldsymbol{\tau}^j \tag{20}$$

where the fourth-order tensor $\boldsymbol{S}^j$ does not depend on $\boldsymbol{\tau}^j$ and is entirely determined from Ω, Ω^j and $\boldsymbol{C}$. It follows that

$$\int_{\Omega^j} \boldsymbol{\varepsilon}^* \mathrm{d}\Omega = |\Omega^j| \left(\boldsymbol{C}^{-1} : \bar{\boldsymbol{\sigma}} + \sum_k \boldsymbol{S}^{jk} : \boldsymbol{\tau}^k \right) \tag{21}$$

where

$$\boldsymbol{S}^{jk} = \frac{1}{|\Omega^j|} \int_{\Omega^j} \boldsymbol{S}^k(\boldsymbol{x}) \mathrm{d}\Omega. \tag{22}$$

For $j \neq k$, the tensor $\boldsymbol{S}^{jk}$ in (22) captures the elastic interaction between grains j and k. The norm of that tensor is expected to decrease with the distance between grains j and k. Substituting (21) in (16) we finally arrive at

$$W = -\frac{1}{2}|\Omega| \bar{\boldsymbol{\sigma}} : \boldsymbol{C}^{-1} : \bar{\boldsymbol{\sigma}} - \sum_j |\Omega^j| \bar{\boldsymbol{\sigma}} : \boldsymbol{\tau}^j - \sum_{j,k} \frac{1}{2} |\Omega^j| \boldsymbol{\tau}^j : \boldsymbol{C} : \boldsymbol{S}^{jk} : \boldsymbol{\tau}^k. \tag{23}$$

Dropping the constant term $|\Omega| \bar{\boldsymbol{\sigma}} : \boldsymbol{C}^{-1} : \bar{\boldsymbol{\sigma}}/2$, minimization problem (11) thus reduces to

$$\begin{aligned} \inf_{\boldsymbol{\gamma}} & -\sum_{j=1}^{M} |\Omega^j| \bar{\boldsymbol{\sigma}} : \boldsymbol{\tau}^j - \sum_{j,k=1}^{M} \frac{1}{2} |\Omega^j| \boldsymbol{\tau}^j : \boldsymbol{C} : \boldsymbol{S}^{jk} : \boldsymbol{\tau}^k + \frac{1}{2} \sum_{j=1}^{M} |\Omega^j| \boldsymbol{\tau}^j : \boldsymbol{C} : \boldsymbol{\tau}^j \\ & + \frac{1}{2} \xi_X \int_{\Omega} \sum_{i=1}^{N} \gamma_i^2 d\Omega + \sum_{i=1}^{N} \int_{\Omega} (\tau_c + \xi \eta_i^0 + \frac{1}{2} \xi \ |\gamma_i - \gamma_i^0|) |\gamma_i - \gamma_i^0| d\Omega. \end{aligned} \tag{24}$$

4.2 Critical grains

Consider an initial state ($t = 0$) in which $\boldsymbol{\gamma} = 0$. In the general case of a non-proportional loading, several slip systems may be successively activated in each grain depending on the direction of $\bar{\boldsymbol{\sigma}}(t)$. However, for a proportional loading as considered in (8), only one slip system is expected to be activated in each grain (at least for small loading level $f(t)$). That slip system $I(j)$ corresponds to the maximum resolved shear stress in each grain, i.e.

$$I(j) = \mathrm{argmax}_{1 \leq i \leq N} |\boldsymbol{\sigma}^0 : \boldsymbol{\tau}_i^j|.$$

Assuming that only slip system $I(j)$ is activated in grain j and denoting by γ^j (resp. η^j) the corresponding plastic slip (resp. cumulated plastic slip), (24) becomes

$$\begin{aligned} \inf_{\boldsymbol{\gamma}} & -\sum_{j} |\Omega^j| \bar{\boldsymbol{\sigma}} : \boldsymbol{\tau}^j - \sum_{j,k} \frac{1}{2} |\Omega^j| \boldsymbol{\tau}^j : \boldsymbol{C} : \boldsymbol{S}^{jk} : \boldsymbol{\tau}^k + \frac{1}{2} \sum_{j} |\Omega^j| \boldsymbol{\tau}^j : \boldsymbol{C} : \boldsymbol{\tau}^j \\ & + \frac{1}{2} \xi_X \sum_{j=1}^{M} |\Omega^j| (\gamma^j)^2 + \sum_{j=1}^{M} |\Omega^j| (\tau_c^0 + \frac{1}{2} \xi \ |\gamma^j - \gamma^{j,0}|) |\gamma^j - \gamma^{j,0}| \end{aligned} \tag{25}$$

where $\gamma^{j,0}$ and $\eta^{j,0}$ are the plastic slip and the accumulated plastic slip in grain j at time t^0. The updated critical shear stress τ_c^0 in (25) is defined by $\tau_c^0 = \tau_c + \xi\eta^{j,0}$. All the grains remains elastic if the loading level $f(t)$ in (8) is such that $|f(t)\boldsymbol{\sigma}^0 : \boldsymbol{\tau}^j_{I(j)}| \leq \tau_c$ for all j, i.e. the elastic limit is

$$\frac{\tau_c}{\sup_j |\boldsymbol{\sigma}^0 : \boldsymbol{\tau}^j_{I(j)}|}.$$

For loading levels slightly above that elastic limit, plastic flow is expected to be limited to few critical grains characterized by the highest value of the resolved shear stress $|\boldsymbol{\sigma}^0 : \boldsymbol{\tau}^j_{I(j)}|$. Without loss of generality, we can assume that those critical grains are grains $1, \cdots, m$. We assume that the critical grains are far away from one another, so that their elastic interaction is negligible. In that case, (24) reduces to

$$\begin{aligned}\inf_{\boldsymbol{\gamma}} -\sum_{j=1}^{m} |\Omega^j| \bar{\boldsymbol{\sigma}} : \boldsymbol{\tau}^j - \sum_{j=1}^{m} \frac{1}{2} |\Omega^j| \boldsymbol{\tau}^j : \boldsymbol{C} : \boldsymbol{S}^{jj} : \boldsymbol{\tau}^j + \frac{1}{2} \sum_{j=1}^{m} |\Omega^j| \boldsymbol{\tau}^j : \boldsymbol{C} : \boldsymbol{\tau}^j \\ + \frac{1}{2} \xi_X \sum_{j=1}^{n} |\Omega^j| (\gamma^j)^2 + \sum_{j=1}^{m} |\Omega^j| (\tau_c^0 + \frac{1}{2}\xi \ |\gamma^j - \gamma^{j,0}|) |\gamma^j - \gamma^{j,0}|\end{aligned} \tag{26}$$

where we recall that $\boldsymbol{\tau}^j = \gamma^j \boldsymbol{\tau}^j_{I(j)}$. Setting

$$\alpha^j = \boldsymbol{\tau}^j_{I(j)} : \boldsymbol{C} : (\boldsymbol{I} - \boldsymbol{S}^{jj}) : \boldsymbol{\tau}^j_{I(j)}, \beta^j = \bar{\boldsymbol{\sigma}} : \boldsymbol{\tau}^j_{I(j)} + \xi\gamma^{j,0}, \tag{27}$$

and

$$\tilde{\alpha}^j = \alpha^j + \xi + \xi_X,$$

the local optimality condition in (26) reads as

$$\beta^j - \tilde{\alpha}^j \gamma^j \begin{cases} \in [-\tau_c^0, \tau_c^0] & \text{if } \gamma^j = \gamma^{j,0} \\ = \tau_c^0 & \text{if } \gamma^j > \gamma^{j,0} \\ = -\tau_c^0 & \text{if } \gamma^j < \gamma^{j,0} \end{cases}$$

which yields

$$\gamma^j = \begin{cases} \gamma^{j,0} & \text{if } |\beta^j - \tilde{\alpha}^j \gamma^{j,0}| \leq \tau_c^0, \\ \dfrac{\beta^j - \tau_c^0}{\tilde{\alpha}^j} & \text{if } \beta^j - \tilde{\alpha}^j \gamma^{j,0} > \tau_c^0, \\ \dfrac{\beta^j + \tau_c^0}{\tilde{\alpha}^j} & \text{if } \beta^j - \tilde{\alpha}^j \gamma^{j,0} < \tau_c^0. \end{cases} \tag{28}$$

for $j = 1, \cdots, m$. The aforementioned assumptions thus allow one to obtain a closed form solution to the incremental problem of elastic-plastic evolutions in a polycrystal. We can observe in (28) that the plastic slips $\gamma^1, \cdots, \gamma^m$ are determined independently from one another, i.e. there is no coupling between the plastifying grains. This results from the fact that the elastic interaction between grains has been neglected. Apart from loading and material parameters, the plastic slip in (28) depend on the shape and the crystalline orientation of the

grain through the scalars α^j and β^j in (27). In more detail, the tensor $\boldsymbol{S}^{jj}$ is determined from the shape of grain j whereas the crystalline orientation plays a role through the selection of the active slip system $I(j)$ and the corresponding strain $\boldsymbol{\tau}^j_{I(j)}$.

5 Illustration

5.1 Mesoscopic model construction

A 2D polycrystalline RVE of 500 grains is generated randomly using *Neper* -a generation and meshing software package based on the Voronoi-Laguerre tessellation. The obtained tessellation is shown in Fig. 1a. The implementation of the formula (28) requires the evaluation of the fourth-order tensor $\boldsymbol{S}^j$ for each grain. Note that problem (19) defining the tensor $\boldsymbol{S}^j$ is formally similar to Eshelby's inclusion problem. However, the irregularity of the grain geometries ruins any hope of solving (19) analytically. Rather than evaluating $\boldsymbol{S}^j$ numerically (which could be done using finite element calculations), we choose to approximate each grain into an ellipsoid, as shown in Fig. 1b . That strategy allows Eshelby's explicit solution [5, 14] to be used for $\boldsymbol{S}^j$. The approximation of each grain into an ellipsoid can be performed using the maximum volume inscribed ellipsoid optimization algorithm in *Matlab* [27] as well as a modeling system for convex optimizations (CVX *Matlab* package).

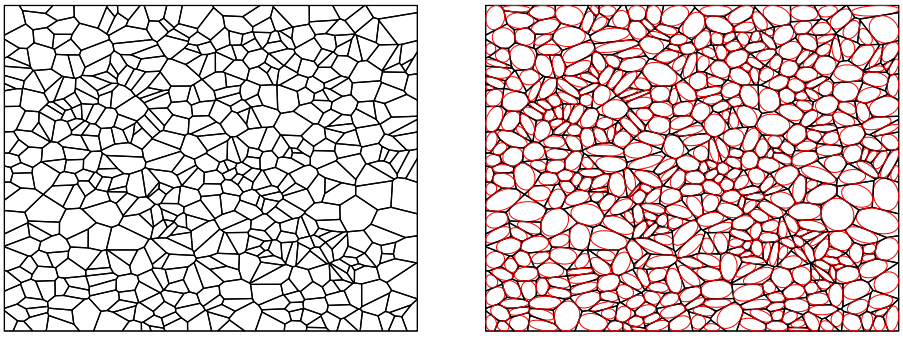

Fig. 1: (a) A 500-grain tessellation generated by *Neper* and (b) its approximated geometry in *Matlab*.

Regarding slip systems, the face-centered cubic lattive (FCC) is one of the most common crystalline structures in metals (Fig. 2a). In that case, there are 12 slip systems defined according to the Thompson tetrahedron. In the 2D setting considered in this paper, we use 6 slip systems defined according to an equilateral triangle shown in Fig. 2b. The inclination angle Θ_j shown in Fig. 2b is the Euler angle describing the crystallographic orientation of grain j. The vectors $(\boldsymbol{n}_i, \boldsymbol{t}_i)$

defining the 6 slip systems in the reference single crystal take the form

$$\begin{cases} \boldsymbol{n}_i = \begin{pmatrix} -\sin(\phi_i) \\ \cos(\phi_i) \end{pmatrix} \text{, where } \phi_i \in \{0°, 60°, 120°\} \\ \\ \boldsymbol{t}_i = \begin{pmatrix} \cos(m_i\phi_i) \\ \sin(m_i\phi_i) \end{pmatrix} \text{, where } m_i \in \{-1, 1\} \end{cases} \tag{29}$$

At this point, all the ingredients are in place for using the simplified model

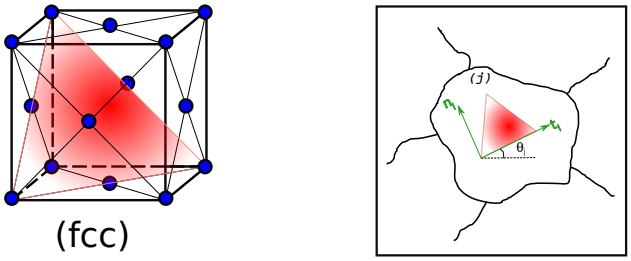

Fig. 2: (a) The FCC crystalline structure. (b) Slip system in grain j of a 2D polycrystal.

presented in Sect. 4: In a first stage, the active slip system and the best fitting ellipsoid are calculated in each grain, which allows one to evaluate the parameters (α^j, β^j) in (27). Subsequently, the plastic slip in each grain is updated at each time step via formula (28).

5.2 Finite element model construction

In order to validate the solution procedure presented in Sect. 4, Finite Element (FE) simulations have been performed in *Freefem++* [7], importing the tessellation shown in Fig. 1a into a 1×1 square domain that was finely meshed. That unit square was embedded into a coarsely meshed 2×2 square serving as an elastic matrix for reducing border effects (Fig. 4a). Material and loading parameters are reported in Table 1. The tensor $\boldsymbol{\sigma}^0$ is set to $(\boldsymbol{u}_1 \otimes \boldsymbol{u}_2 + \boldsymbol{u}_2 \otimes \boldsymbol{u}_1)/2$ (pure shear). The plastic slip at each Gauss point is calculating using Lemke's algorithm [3] for solving the linear complementarity problem arising from (11). In Fig. 4a are shown the plastic slips as calculated by the finite element method after the first half-cycle. An average plastic slip per grain has been extracted from the FE simulations and compared with the results obtained from the formula (28). The relative error between those two values has been calculated for each grain and is shown in Fig. 4b as a function of the average plastic slip computed in *Freefem++*. The average relative error is 4.46% (4.28% when restricted

E (GPa)	ν	f^a (MPa)	f^m (MPa)	ζ/μ (MPa^{-1})	τ_c^0 (MPa)
210	0.3	101	0	1615.38	100

Table 1: Material and loading parameters

to the critical grains with the highest plastic slips as shown in Fig. 4b) with a maximum of approximately 13% (7% when restricted to critical grains). A finer meshing density reduces the average error on critical grains to 3.79%. That error is partly due to the nonuniformity of the plastic slip within each grain, the elastic interaction between plastifying grains and the irregularity of the grain geometries, all of which are not taken into account in the simplified method.

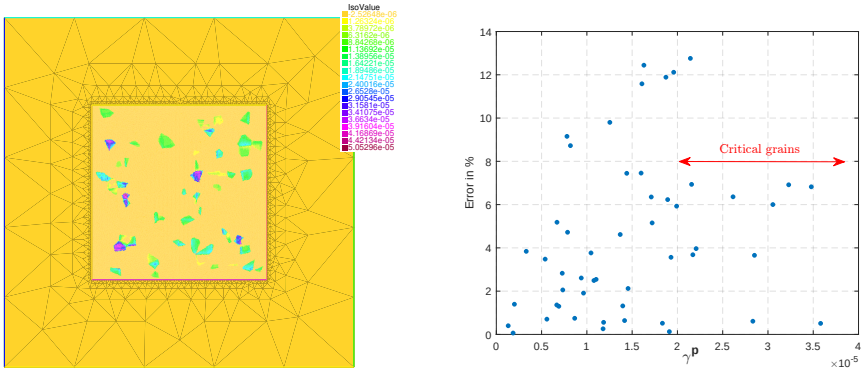

(a) FE results for the plastic slip field in the polycrystal

(b) Model error as a function of the plastic slip (FE value)

Fig. 3: Validation of the mesoscopic model.

6 Direct approach for cyclic loadings

The simplified method presented in Sect. 4 allows one to estimate the step-by-step evolution of plastic slips for a given loading history. In this Section, we consider a cyclic loading and are interested in the asymptotic state reached by the polycrystal as the number of cycles grows to infinity. As detailed in the following, we show that asymptotic values of the plastic slips (and cumulated plastic slips) in each grain can be obtained directly, i.e without carrying out step-by-step calculations. Since there is no coupling between grains in (28), we first note that critical grains can studied independently from one another. Hence, from now on we simplify the notations by dropping the superscript j in (28) and consider a single critical grain. The active slip system is denoted by $(\boldsymbol{n}, \boldsymbol{t})$. We

have

$$\gamma = \begin{cases} \gamma^0 & \text{if } |\beta - \tilde{\alpha}\gamma^0| \leq \tau_c^0 \\ \dfrac{\beta - \tau_c^0}{\tilde{\alpha}} & \text{if } \beta - \tilde{\alpha}\gamma^0 > \tau_c^0 \\ \dfrac{\beta + \tau_c^0}{\tilde{\alpha}} & \text{if } \beta - \tilde{\alpha}\gamma^0 < \tau_c^0 \end{cases} \tag{30}$$

where

$$\alpha = \boldsymbol{\tau} : \boldsymbol{C} : (\boldsymbol{I} - \boldsymbol{S}) : \boldsymbol{\tau}, \quad \beta = \bar{\boldsymbol{\sigma}} : \boldsymbol{\tau} + \xi\gamma^0, \tag{31}$$

and

$$\boldsymbol{\tau} = \frac{1}{2}(\boldsymbol{t} \otimes \boldsymbol{n} + \boldsymbol{n} \otimes \boldsymbol{t}), \quad \tilde{\alpha} = \alpha + \xi + \xi_X.$$

We consider a cyclic loading of the form (8) where $f(t)$ alternates between a minimum value f_{min} and a maximum value f_{max}. To fix ideas, we assume that $f(0) = f(T) = f_{min}$ and $f(T/2) = f_{max}$ where T is the period of the loading. The function f is monotonically increasing (resp. decreasing) on the time interval $[0, T/2]$ (resp. $[T/2, T]$) and the plastic slip γ is expected to have a similar behavior. This motivates calculating the evolution of γ by solving the incremental problem (28) on each of the half-cycles $[nT, nT + T/2]$ and $[nT + T/2, (n+1)T]$. We denote by γ_n (resp. $\gamma_{n+\frac{1}{2}}$) the value of γ at time nT (resp $nT + T/2$). Similarly we denote by $\tau_{c,n}$ (resp. $\tau_{c,n+\frac{1}{2}}$) the value of the updated critical shear stress τ_c at time nT (resp $nT + T/2$). We obtain

$$\gamma_{n+\frac{1}{2}} = \begin{cases} \gamma_n & \text{if } |\beta_{n+\frac{1}{2}} - \tilde{\alpha}\gamma_n| \leq \tau_{c,n} \\ \dfrac{\beta_{n+\frac{1}{2}} - \tau_{c,n}}{\tilde{\alpha}} & \text{if } \beta_{n+\frac{1}{2}} - \tilde{\alpha}\gamma_n > \tau_{c,n} \end{cases} \tag{32}$$

where $\beta_{n+\frac{1}{2}} = f_{max}\boldsymbol{\sigma}^0 : \boldsymbol{\tau} + \xi\gamma_n$, and

$$\gamma_{n+1} = \begin{cases} \gamma_{n+\frac{1}{2}} & \text{if } |\beta_{n+1} - \tilde{\alpha}\gamma_{n+\frac{1}{2}}| \leq \tau_{c,n+\frac{1}{2}} \\ \dfrac{\beta_{n+1} + \tau_{c,n+\frac{1}{2}}}{\tilde{\alpha}} & \text{if } \beta_{n+1} - \tilde{\alpha}\gamma_{n+\frac{1}{2}} < \tau_{c,n+\frac{1}{2}} \end{cases} \tag{33}$$

where $\beta_{n+1} = f_{min}\boldsymbol{\sigma}^0 : \boldsymbol{\tau} + \xi\gamma_{n+\frac{1}{2}}$. Formulas (32) and (33) give a recurrence relation for calculating the sequence of plastic slips $\gamma_1, \gamma_2, \cdots$. Let us consider the case where shakedown occurs, i.e. the plastic slip converge towards a time-independent value γ_∞ as time tends to infinity. Taking the limit $n \to \infty$ in (32)-(33) and assuming plastic flow on each half-cycle, we obtain the relations

$$\begin{aligned} \gamma_\infty &= \frac{f_{max}\boldsymbol{\sigma}^0 : \boldsymbol{\tau} + \xi\gamma_\infty - \tau_{c,\infty}}{\tilde{\alpha}} \\ \gamma_\infty &= \frac{f_{min}\boldsymbol{\sigma}^0 : \boldsymbol{\tau} + \xi\gamma_\infty + \tau_{c,\infty}}{\tilde{\alpha}} \end{aligned} \tag{34}$$

where $\tau_{c,\infty} = \tau_c + \xi\eta_\infty$ and $\eta_\infty = \displaystyle\sum_{n=0}^{\infty}(|\gamma_{n+1} - \gamma_{n+\frac{1}{2}}| + |\gamma_{n+\frac{1}{2}} - \gamma_n|)$ is the asymptotic value of the cumulated plastic slip. It follows that

$$\gamma_\infty = \boldsymbol{\sigma}^0 : \boldsymbol{\tau}\frac{f_{max} + f_{min}}{2(\alpha + \xi_X)}, \quad \tau_{c,\infty} = \boldsymbol{\sigma}^0 : \boldsymbol{\tau}\frac{f_{max} - f_{min}}{2} \tag{35}$$

from which we obtain the value of η_∞ as

$$\eta_\infty = \frac{1}{\xi}(\frac{f_{max}-f_{min}}{2}\boldsymbol{\sigma}^0 : \boldsymbol{\tau} - \tau_c). \tag{36}$$

The obtained expressions for γ_∞ and η_∞ can be rewritten in a more compact fashion as

$$\gamma_\infty = \frac{\sigma^m_{nt}}{\alpha + \xi_X},\ \eta_\infty = \frac{\sigma^a_{nt} - \tau_c}{\xi} \tag{37}$$

where

$$\sigma^m_{nt} = \frac{f_{max}+f_{min}}{2}\boldsymbol{\sigma}^0 : \boldsymbol{\tau}, \sigma^a_{nt} = \frac{f_{max}-f_{min}}{2}\boldsymbol{\sigma}^0 : \boldsymbol{\tau} \tag{38}$$

are respectively the mean value and the amplitude of the resolved macroscopic stress $f(t)\boldsymbol{\sigma}^0 : \boldsymbol{\tau}$. Formula (37) shows that there is a simple relation between the loading parameters and the plastic state variables in the shakedown state. However, there are some restrictions on the loading parameters for that formula to apply. We have indeed

$$|\gamma_\infty| = |\sum_{n=0}^{\infty}(\gamma_{n+1}-\gamma_{n+\frac{1}{2}})+(\gamma_{n+\frac{1}{2}}-\gamma_n)| \leq \sum_{n=0}^{\infty}|\gamma_{n+1}-\gamma_{n+\frac{1}{2}}|+|\gamma_{n+\frac{1}{2}}-\gamma_n| = \eta_\infty$$

which implies that (37) holds only if

$$\frac{|\sigma^m_{nt}|}{\alpha+\xi_X} \leq \frac{\sigma^a_{nt}-\tau_c}{\xi}. \tag{39}$$

When the loading parameters $(\sigma^m_{nt}, \sigma^a_{nt})$ do not satisfy that condition, shakedown is found to occur after a finite number of cycles. There is no direct formula for estimating the shakedown state in that case.

Expressions (37) for the asymptotic state are verified through a comparison with a step-by-step simulation of a 100-grain randomly generated tessellation submitted to a cyclic shear. In Fig. 4a is shown the plastic slip γ_{Nc} as a function of N_c, as calculated from (30). The cumulated slip η_{Nc} is shown in Fig. 4b. Those values correspond to the grain that plastifies first in the tessellation. The material and loading parameters used are reported in Table 2. The values γ_∞ and η_∞ given by (37) are shown as red lines in Fig. 4. As expected, (γ_{Nc}, η_{Nc}) converge towards γ_∞ and η_∞ as $N_c \to \infty$. For $N_c > 1.1\,10^6$, the relative difference between γ_{Nc} and γ_∞ is smaller than 1% .

E (GPa)	ν	f^a (MPa)	f^m (MPa)	ζ (MPa^{-1})	τ_c^0 (MPa)
210	0.3	101	50	5.10^{-2}	90

Table 2: Material and loading parameters

Formulas (37) gives a direct approach for estimating the asymptotic state in each grain of the polycrystal. This is valuable for fatigue analysis and probabilistic studies, as illustrated in the next Sections.

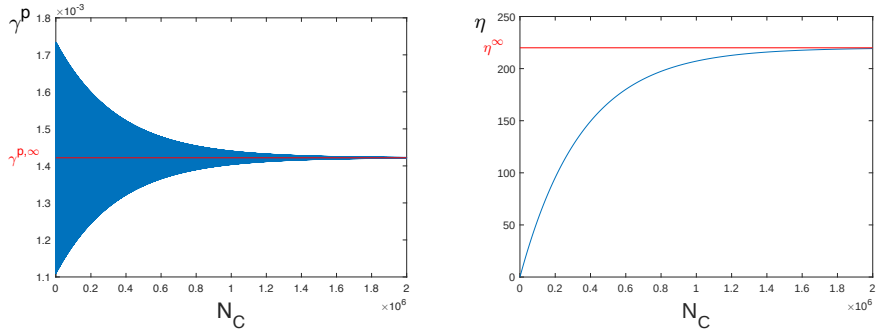

(a) Plastic slip as a function of the number of cycles

(b) Cumulated plastic slip as a function of the number of cycles

Fig. 4: Asymptotic state in a critical grain.

7 Mesoscopic fatigue criterion

Experimental observations show that fatigue cracks usually appear in persistent slip bands inside critical grains. Motivated by such observations, we consider that a fatigue crack may initiate in a given critical grain if $X \geq b$ where

$$X = \sup_t \sigma_{nt}(t) + a\sigma_{nn}(t) \tag{40}$$

and (a, b) are (positive) material parameters. In (40), $\sigma_{nt}(t)$ and $\sigma_{nn}(t)$ are defined as

$$\sigma_{nt}(t) = \boldsymbol{n} \cdot \boldsymbol{\sigma}(t) \cdot \boldsymbol{t}, \quad \sigma_{nn}(t) = \boldsymbol{n} \cdot \boldsymbol{\sigma}(t) \cdot \boldsymbol{n}$$

where $\boldsymbol{n}$ is the normal to the active slip plane, $\boldsymbol{t}$ is the direction of the slip and $\boldsymbol{\sigma}(t)$ is the local stress in the shakedown state. Correspondingly, fatigue life is infinite if

$$X \leq b. \tag{41}$$

A condition similar to (41) is considered in Dang Van's fatigue criterion [4] and is also related to damage indicators proposed by [13]. In the original construction of Dang Van's fatigue criterion, the purely elastic stress in critical grains is approximated using Lin-Taylor's approximation and the stabilized plastic strain is estimated using a heuristic ansatz. The approach presented allows one to improve on those assumptions. In more detail, when shakedown is reached in a critical grain, the local stress takes the form

$$\boldsymbol{\sigma}(t) = \bar{\boldsymbol{\sigma}}(t) - \gamma_\infty \boldsymbol{C} : (\boldsymbol{I} - \boldsymbol{S}) : \boldsymbol{\tau}.$$

Recalling that $\boldsymbol{C}$ is isotropic (with Lame coefficients (λ, μ)) and noting that $\boldsymbol{n} \cdot \boldsymbol{t} = 0$, we have

$$\sigma_{nt}(t) = f(t)\sigma^0_{nt} - \gamma_\infty \alpha, \ \sigma_{nn}(t) = f(t)\sigma^0_{nn} - \gamma_\infty \alpha' \tag{42}$$

where α is defined as in (31) and

$$-\alpha' = \lambda \operatorname{tr}(\boldsymbol{S} : \boldsymbol{\tau}) + 2\mu \boldsymbol{n} \otimes \boldsymbol{n} : \boldsymbol{S} : \boldsymbol{\tau}. \tag{43}$$

In (42), we have set $\sigma^0_{nt} = \boldsymbol{n} \cdot \boldsymbol{\sigma}^0 \cdot \boldsymbol{t}$ and $\sigma^0_{nn} = \boldsymbol{n} \cdot \boldsymbol{\sigma}^0 \cdot \boldsymbol{n}$. Using expression (37) for γ_∞ yields

$$\sigma_{nt}(t) + a\sigma_{nn}(t) = f(t)(\sigma^0_{nt} + a\sigma^0_{nn}) - (\alpha + a\alpha')\frac{\sigma^m_{nt}}{\alpha + \xi_X}.$$

The value of $f(t)$ reaching the maximum of the expression above is either f_{max} or f_{min}, depending on the sign of $\sigma^0_{nt} + a\sigma^0_{nn}$. Setting

$$\sigma^m_{nn} = \frac{f_{max} + f_{min}}{2}\sigma^0_{nn}, \sigma^a_{nn} = \frac{f_{max} - f_{min}}{2}\sigma^0_{nn}, \tag{44}$$

we arrive at $X = \sup\{X_+, X_-\}$ where

$$X_\pm = \sigma^m_{nt} + a\sigma^m_{nn} \pm (\sigma^a_{nt} + a\sigma^a_{nn}) - (\alpha + a\alpha')\frac{\sigma^m_{nt}}{\alpha + \xi_X}. \tag{45}$$

In the case $\xi_X = 0$ (which we consider in the following), the expression above simplifies as

$$X_\pm = a\sigma^m_{nn} \pm (\sigma^a_{nt} + a\sigma^a_{nn}) - a\frac{\alpha'}{\alpha}\sigma^m_{nt}. \tag{46}$$

7.1 Influence of the grain shape

The quantity $X = \sup\{X_+, X_-\}$ drives the fatigue life of critical grains. For a given loading, X depends on the shape of critical grains through the ratio α'/α where α and α' are defined in (31) and (43) respectively. That ratio can be interpreted as a geometric amplification factor of the mean resolved shear stress σ^m_{nt}. Evaluating α'/α requires evaluating the tensor $\boldsymbol{S}$ introduced in (20), which can only be done numerically in general. A notable exception is the case of ellipsoidal grains, for which $\boldsymbol{S}$ coincides with the Eshelby tensor. Let $r \leq 1$ be the aspect ratio of the ellipsoidal grain and let x be the angle between the long axis of the grain and the direction $\boldsymbol{n}$ of the slip plane. Some calculations based on the expression of the Eshelby tensor leads to

$$\frac{-\alpha'}{\alpha} = \frac{2(1-r)(1+r+(1-r)\cos 2x)\sin 2x}{(1+r)^2 - (1-r)^2\cos 4x}. \tag{47}$$

Interestingly, the ratio $-\alpha'/\alpha$ is found to be independent of the elastic moduli. It is plotted in Fig. 5(left) as a function of the angle x, for several values of the aspect ratio r. In the limit case $r = 1$ (circular inclusion), α'/α is equal to 0. In the limit case $r = 0$ (flat grains), we obtain $-\alpha'/\alpha = \operatorname{cotan} x$ which may take any value in $\mathbb{R}$ depending on the angle x. We have in particular $-\alpha'/\alpha = +\infty$ when $x = 0$, i.e. when the normal to slip plane is parallel to the (flat) grain. More generally, for a given aspect ratio r, it can easily be seen that $-\alpha'/\alpha$ is $\pi-$periodic and covers an interval of the form $[-M(r), M(r)]$ as x varies between 0 and π. The function $M(r)$ is plotted in Fig. 5(right) and can be interpreted as a maximum amplification factor of σ^m_{nt} in the fatigue life indicator X.

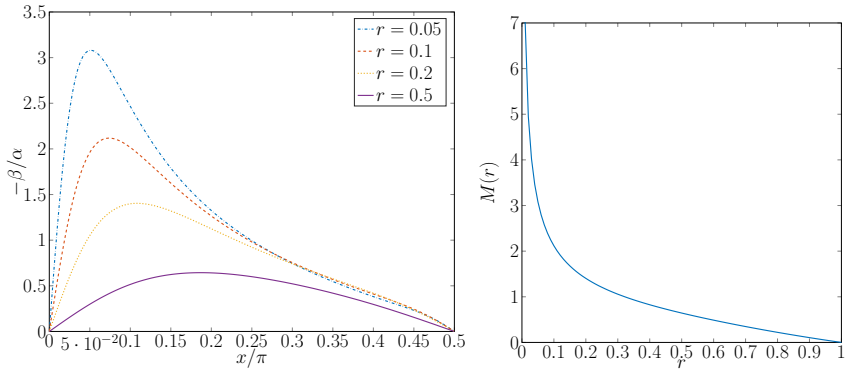

Fig. 5: Geometric amplification factor capturing the influence of the grain shape (orientation x, aspect ratio r) on the fatigue indicator.

7.2 Influence of the crystalline orientation

For a given aspect ratio r, we consider the worst situation where the angle x gives the largest value of $|\alpha'/\alpha|$ in which case

$$X_{\pm} = a\sigma^m_{nn} \pm (\sigma^a_{nt} + a\sigma^a_{nn}) + aM(r)|\sigma^m_{nt}|.$$

Let $(\boldsymbol{u}_1, \boldsymbol{u}_2)$ be eigenvectors of $\boldsymbol{\sigma}^0$, so that $\boldsymbol{\sigma}^0 = \lambda_1 \boldsymbol{u}_1 \otimes \boldsymbol{u}_1 + \lambda_2 \boldsymbol{u}_2 \otimes \boldsymbol{u}_2$ with $\lambda_1 \leq \lambda_2$. The orientation θ of the active slip system depends on the crystalline orientation and can be parameterized by the angle θ such that $\boldsymbol{n} = \cos\theta \boldsymbol{u}_1 + \sin\theta \boldsymbol{u}_2$ and $\boldsymbol{t} = -\sin\theta \boldsymbol{u}_1 + \cos\theta \boldsymbol{u}_2$. We have

$$\begin{aligned} X_+ = a(f^m + f^a)(\lambda_2 + (\lambda_1 - \lambda_2)(\cos\theta)^2) + f^a(\lambda_2 - \lambda_1)\sin\theta\cos\theta \\ + aM(r)|f^m|(\lambda_2 - \lambda_1)|\sin\theta\cos\theta| \end{aligned} \tag{48}$$

where

$$f^m = \frac{f_{max} + f_{min}}{2}, \quad f^a = \frac{f_{max} - f_{min}}{2}.$$

The most critical value of X_+ is obtained by maximization with respect to θ. That maximization can be performed in closed form (details omitted) yielding

$$\sup_\theta X_+ = a(f^m + f^a)\frac{\lambda_1 + \lambda_2}{2} + \frac{1}{2}(\lambda_2 - \lambda_1)\sqrt{(f^a + aM(r)|f^m|)^2 + a^2(f^m + f^a)^2}.$$

A similar calculation gives

$$\sup_\theta X_- = a(f^m - f^a)\frac{\lambda_1 + \lambda_2}{2} + \frac{1}{2}(\lambda_2 - \lambda_1)\sqrt{(f^a + aM(r)|f^m|)^2 + a^2(f^m - f^a)^2}.$$

Hence, if

$$a(f^m \pm f^a)\frac{\lambda_1 + \lambda_2}{2} + \frac{1}{2}(\lambda_2 - \lambda_1)\sqrt{(f^a + aM(r)|f^m|)^2 + a^2(f^m \pm f^a)^2} \leq b \tag{49}$$

then a critical grain of aspect ratio r satisfies the infinite lifetime condition, whatever its geometric or crystalline orientation. Now consider a polycrystal made of ellipsoidal grains with varying aspect ratios in a given interval $[r_0, r_1]$. Observing that the left-hand side of (49) is increasing with $M(r)$ and noting from Fig. 5(right) that M is decreasing with r, we obtain that the condition

$$a(f^m \pm f^a)\frac{\lambda_1+\lambda_2}{2}+\frac{1}{2}(\lambda_2-\lambda_1)\sqrt{(f^a+aM(r_0)|f^m|)^2+a^2(f^m\pm f^a)^2} \leq b \quad (50)$$

ensures that all critical grains satisfy the infinite lifetime condition, whatever their orientation (both geometric and crystalline) and whatever the exact value of their aspect ratios. Condition (50) can thus be interpreted as an infinite lifetime condition for the polycrystal. It is expected to be representative of polycrystals that contains many grains covering almost all possible orientations. In that case, there is indeed a high probability that there exists a critical grain close to the worst orientation, thus achieving the value $\max X$ in (50). For a RVE with few grains or a with special texture, condition (50) is expected to be conservative. More details on such issues are provided in Sect. 8.

In condition (50), the only parameters related to the shape of the grains is the scalar $M(r_0)$. The most favorable situation corresponds to circular inclusions ($r_0 = 1$), in which case $M(r_0) = 0$ and (50) reduces to

$$a(f^m \pm f^a)\frac{\lambda_1+\lambda_2}{2} + \frac{1}{2}(\lambda_2-\lambda_1)\sqrt{(f^a)^2+a^2(f^m\pm f^a)^2} \leq b. \quad (51)$$

Eq. (51) is expressed only in terms of macroscopic loading parameters. It can be interpreted as an upscaled version of the local expression (41) used in individual grains. It is interesting to compare (50) with 2D versions of widely used macroscopic fatigue criteria such as Crossland's, Sines' or Dang Van's criterion. For the loading considered, the infinite lifetime condition obtained from a 2D version of Dang Van's criterion takes the form

$$a(f^m \pm f^a)\frac{\lambda_1+\lambda_2}{2} + \frac{1}{2}(\lambda_2-\lambda_1)f^a \leq b. \quad (52)$$

There is a close resemblance between (52) and (50), especially in the case of circular grains. In particular, the term in $\frac{\lambda_1+\lambda_2}{2}$ is the same. Condition (51) can be observed to be more conservative than (52) because the multiplying factor of $\frac{\lambda_2-\lambda_1}{2}$ is larger. The infinite lifetime condition obtained from Crossland's and Sines' criteria in 2D read respectively as

$$a(f^m\frac{\lambda_1+\lambda_2}{2} + f^a|\frac{\lambda_1+\lambda_2}{2}|) + \frac{1}{2}(\lambda_2-\lambda_1)f^a \leq b \quad (53)$$

$$af^m\frac{\lambda_1+\lambda_2}{2} + \frac{1}{2}(\lambda_2-\lambda_1)f^a \leq b \quad (54)$$

which differ from (52) by the term in $(\lambda_1+\lambda_2)/2$ capturing the influence of the hydrostatic stress. In Dang Van's, Crossland's and Sines' criterion, the term in $(\lambda_2-\lambda_1)/2$ (capturing the influence of the deviatoric stress) is the same.

8 Probabilistic aspects

8.1 Survival function for a critical grain of random orientation

The direct expressions (37) for the asymptotic state are well suited to a probabilistic analysis of fatigue. This Section elaborates on this point for the simplest case of a zero-mean loading (i.e $f^m = 0$) and circular grains. In that case, we have from (48)

$$X_+ = -X_- = af^a(\lambda_2 + (\lambda_1 - \lambda_2)(\cos\theta)^2) + f^a(\lambda_2 - \lambda_1)\sin\theta\cos\theta \qquad (55)$$

where we recall that θ is the orientation of the active slip system. The angle θ depends on the crystalline orientation Θ in the critical grain, as shown in Fig. 6 for the case of the 6 slip systems listed in (29). In that case, it can be calculated that $\theta = \Theta - \pi/3$ if $0 \leq \Theta \leq \pi/6$ (modulo $\pi/2$), $\theta = \Theta$ if $\pi/6 \leq \Theta \leq \pi/3$ (modulo $\pi/2$), $\theta = \Theta + \pi/3$ if $\pi/3 \leq \Theta \leq \pi/2$ (modulo $\pi/2$). Setting $\psi = \arctan(1/a)$,

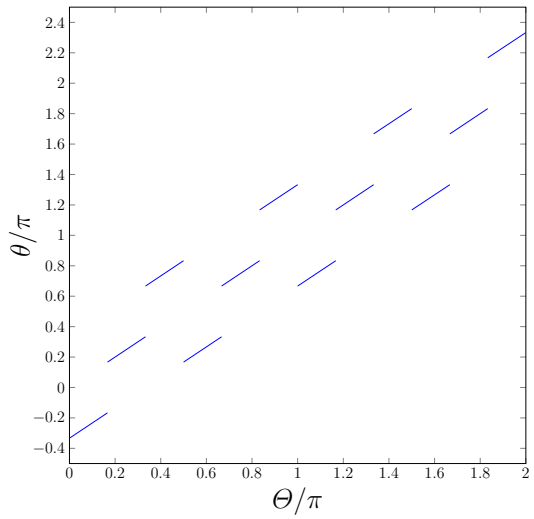

Fig. 6: Angle θ of the active slip system as a function of the crystalline orientation Θ.

some straightforward manipulations lead to

$$\frac{X_+}{f^a} = a\frac{\lambda_1 + \lambda_2}{2} + \sqrt{1 + a^2}\frac{\lambda_1 - \lambda_2}{2}y \qquad (56)$$

where

$$y = \cos(2\theta + \psi). \qquad (57)$$

Provided that $\pi/6 \leq \psi \leq \pi/3$ (which corresponds to a in the range $[1/\sqrt{3}, \sqrt{3}]$), it can be verified that y takes values in $[-y_2, -y_1] \cup [y_1, y_2]$ where

$$y_1 = \cos(\psi - \frac{2\pi}{3}), \quad y_2 = \cos(\psi - \frac{\pi}{3}).$$

If now Θ is seen as a random variable with a prescribed probability density, then relations (56) and (57) allow one to calculate the probability densities of y and $X = \max(X_+, X_-)$. In the particular case where Θ is uniformly distributed on $[0, 2\pi]$, it can be calculated that the variable y has a probability density p given by

$$p(y) = \begin{cases} \dfrac{3}{2\pi} \dfrac{1}{\sqrt{1-y^2}} & \text{if } |y| \in [y_1, y_2], \\ 0 & \text{otherwise.} \end{cases} \tag{58}$$

The probability density p in (58) is shown in Fig. 7 (red curve). To validate

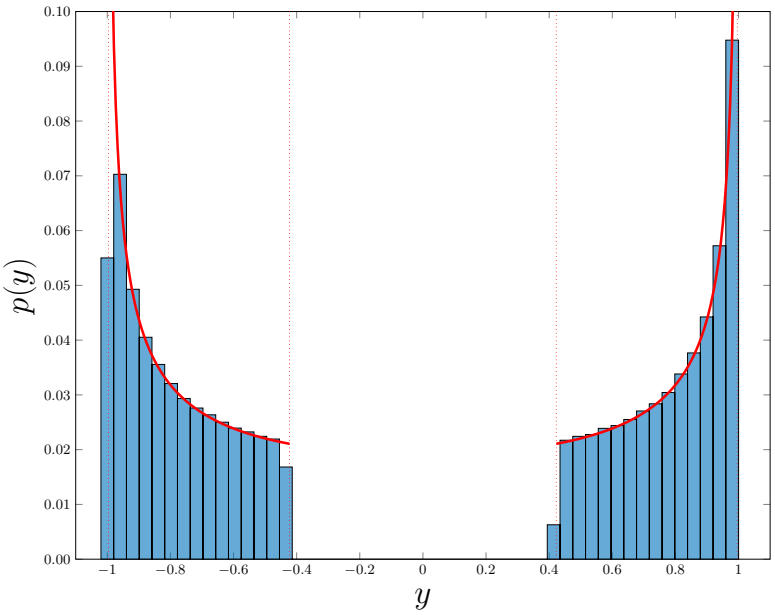

Fig. 7: Probability density p of $y = \cos 2\theta + \psi$ (red curve). The vertical dashed lines show the support of p. The histogram shows the probability density approximated from a sample of 1000000 randomly generated crystalline orientations.

expression (58), the values of y corresponding to 1000000 randomly generated crystalline orientations have been calculated. The results, shown as a normalized histogram in Fig. 7, are in good agreement with (58).

The probability density of X can be obtained from (58) and relation (55). Of particular interest is the survival function for X, defined as the probability

that $X \leq b$ when f^a is prescribed. That quantity is denoted by $S(f^a)$ in the following. It can be interpreted as the probability of infinite lifetime for a critical grain of random orientation when submitted to a loading amplitude f^a. Eq. (56) shows that the condition $X \leq b$ is equivalent to

$$\frac{1}{B}(A - \frac{b}{f_a}) \leq y \leq \frac{1}{B}(A + \frac{b}{f_a})$$

where

$$A = a\frac{\lambda_1 + \lambda_2}{2},\ B = \sqrt{1+a^2}\frac{\lambda_2 - \lambda_1}{2}. \tag{59}$$

It follows that

$$S(f^a) = \int_{\frac{A-b/f^a}{B}}^{\frac{A+b/f^a}{B}} p(y)dy. \tag{60}$$

Using expression (58) for p, there is no substantial difficulty in evaluating the integral in (60). The result depends on the loading mode $\boldsymbol{\sigma}^0$ in (8) through the parameters (A, B) in (59). Both those parameters depend indeed on the eigenvalues (λ_1, λ_2) of $\boldsymbol{\sigma}^0$. Let us consider the case of pure shear, i.e. $\boldsymbol{\sigma}^0 = (\boldsymbol{u}_1 \otimes \boldsymbol{u}_2 + \boldsymbol{u}_2 \otimes \boldsymbol{u}_1)/2$. In that case we have $A = 0$, $B = \sqrt{1+a^2}$ and we obtain

$$S(f^a) = \begin{cases} 0 & \text{if } f_a \geq \dfrac{b}{y_1\sqrt{1+a^2}} \\ \dfrac{1}{2} + \dfrac{3}{\pi}(\arcsin(\dfrac{b}{f^a\sqrt{1+a^2}}) - \psi) & \text{if } \dfrac{b}{y_2\sqrt{1+a^2}} \leq f^a \leq \dfrac{b}{y_1\sqrt{1+a^2}} \\ 1 & \text{if } f_a \leq \dfrac{b}{y_2\sqrt{1+a^2}} \end{cases} \tag{61}$$

The survival function given by (61) is plotted in Fig. 8 for the case $a = 0.7$. For any given k in $[0, 1]$, we denote by f^a_k the maximum loading amplitude f^a such that $S(f^a) = k$. It can be verified from (61) that the median survival loading $f^a_{50\%}$ (i.e. the loading f^a corresponding to a survival probability of 50%) is equal to b. The value $f^a_{100\%}$ (corresponding to a guaranteed infinite lifetime) is equal to $b/y_2\sqrt{1+a^2}$, with $y_2 \simeq 0.996$ for the case $a = 0.7$ depicted in Fig. 8. It is interesting to compare that value with the maximum value f^a_{meso} corresponding to an infinite lifetime according to the mesoscopic fatigue criterion (50). For the loading under consideration, we obtain from (50) that $f^a_{meso} = b/\sqrt{1+a^2}$ which is slightly smaller that $f^a_{100\%}$. The reason is that Eq. (50) was derived by allowing the orientation θ of the active slip system to take any value in $[0, 2\pi]$, which is actually not the case as shown in Fig. 6. However, the relative difference between $f^a_{100\%}$ and f^a_{meso} is really small in the case $a = 0.7$ (this can be verified to remain true for any value of a in $[0, 1]$).

8.2 Survival function for a RVE with M critical grains

Consider now a RVE containing M critical grains and submitted to a given macroscopic loading $(f^m, f^a, \boldsymbol{\sigma}^0)$. The RVE survives (i.e. has an infinite time) is

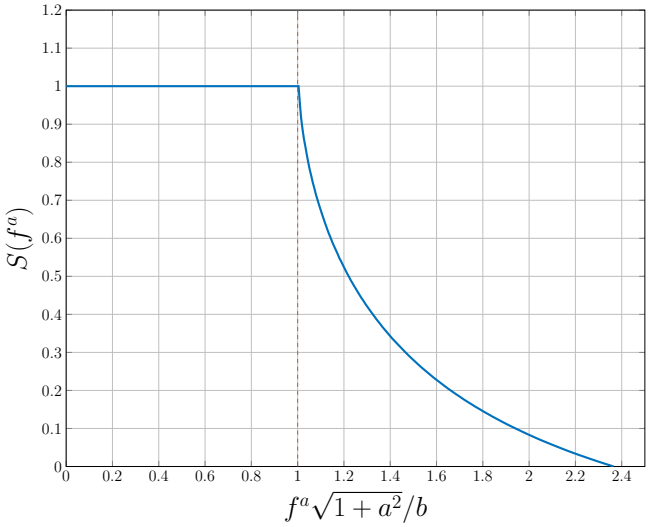

Fig. 8: Survival function for a critical grain of random orientation. Case $f^m = 0$, $\boldsymbol{\sigma}^0 = (\boldsymbol{u}_1 \otimes \boldsymbol{u}_2 + \boldsymbol{u}_2 \otimes \boldsymbol{u}_1)/2$, $a = 0.7$.

all its critical grains do. If the crystalline orientations in the critical grains are statically independent variables, the survival function S_{meso} of the RVE is

$$S_{meso} = S^M \tag{62}$$

In (62) it is assumed implicitly that all the critical grains have the same survival function S, which is notably the case if $f^m = 0$ and the grains are circular. For a shear loading with zero-mean value ($\boldsymbol{\sigma}^0 = (\boldsymbol{u}_1 \otimes \boldsymbol{u}_2 + \boldsymbol{u}_2 \otimes \boldsymbol{u}_1)/2$, $f^m = 0$), it follows from (61) and (62) that the loading amplitude $f^a_{50\%}$ corresponding to a 50% probability of survical for the RVE is

$$\frac{b}{\sqrt{1+a^2}} \frac{1}{\sin(\psi + \frac{\pi}{6}(2^{1-\frac{1}{M}} - 1))}. \tag{63}$$

The value $f^a_{50\%}$ given by (63) is plotted in Fig. 9 as a function of the number M of critical grains. It can be verified that $f^a_{50\%}$ converges towards $b/y_2\sqrt{1+a^2} \simeq f^a_{meso}$ as $M \to \infty$. This means that the mesoscopic criterion (50) is a good fatigue indicator for RVE with many critical grains. In fact, 20 critical grains is enough for the relative difference between $f^a_{50\%}$ and f^a_{meso} to be smaller than 1%. By contrast, for a RVE with a small number (<10) of critical grains, $f^a_{50\%}$ may be significantly larger than f^a_{meso}. Such a situation may occur for structures with large stress gradients. In that case, the stress field varies rapidly in space, which imposes the RVE to be small, consequently reducing the potential number of critical grains. This in accordance with the experimental observation that fatigue limits generally increase in the presence of local stress gradients [12, 11].

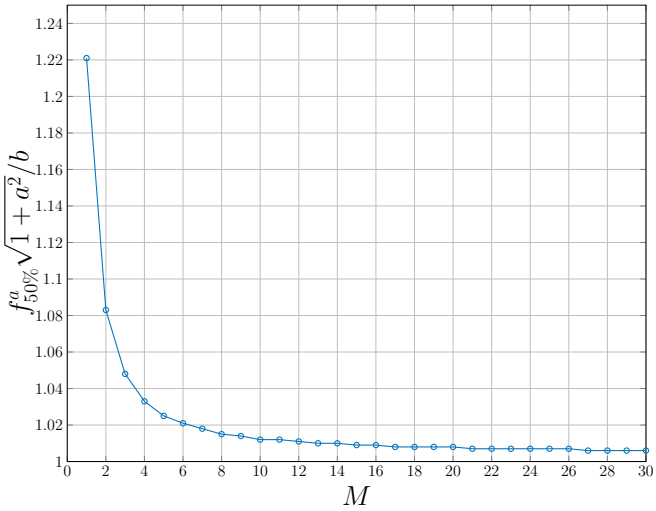

Fig. 9: Median loading amplitude $f^a_{50\%}$ for a RVE with M critical grains. Case $f^m = 0$, $\boldsymbol{\sigma}^0 = (\boldsymbol{u}_1 \otimes \boldsymbol{u}_2 + \boldsymbol{u}_2 \otimes \boldsymbol{u}_1)/2$, $a = 0.7$.

9 Concluding remarks

In this paper we have presented a simplified method for calculating the elastic-plastic evolutions of polycrystals submitted to loadings of relatively low amplitude. The comparison with full-field FE simulations shows that the method presented is relatively accurate, at least in situations where plastifying grains are relatively far away from each other. The main advantage of the proposed approach lies in its numerically efficiency as it relies on analytical formula. In the case of cyclic loadings, the proposed approach leads to a direct method for estimating the asymptotic state. The proposed approach could be extended in several ways. For instance, more advanced hardening laws could be considered. The accuracy of the method could also be improved by taking the elastic interaction between critical grains into account, which is the topic of ongoing work. An other important issue is the extension to the 3D setting. In that regard, we note that the simplified model of Sect. 4 and the analytical formula of Sect. 6 for the shakedown state can be directly extended to 3D. However, the construction of the mesoscopic fatigue criterion in Sect. 7 as well as the probabilistic analysis in Sect. 8 should be revisited and involve more complex calculations.

References

1. Bertolino, G., Constantinescu, A., Ferjani, M., Treiber, P.: A multiscale approach of fatigue and shakedown for notched structures. Theoretical and Applied Fracture Mechanics **48**(2), 140–151 (2007)

2. Bluthé, J., Weisz-Patrault, D., Ehrlacher, A.: Energetic approach for a sliding inclusion accounting for plastic dissipation at the interface, application to phase nucleation. International Journal of Solids and Structures **121**, 163–173 (2017), https://doi.org/10.1016/j.ijsolstr.2017.05.023
3. Cottle, R.W., Pang, J.S., Stone, R.E.: The linear complementarity problem. SIAM (2009)
4. Dang Van, K.: Introduction to fatigue analysis in mechanical design by the multiscale approach. In: High-cycle metal fatigue, pp. 57–88. Springer (1999)
5. Eshelby, J.D.: The determination of the elastic field of an ellipsoidal inclusion, and related problems. In: Proceedings of the Royal Society of London A: Mathematical, Physical and Engineering Sciences. vol. 241, pp. 376–396. The Royal Society (1957)
6. Halphen, B., Nguyen, Q.S.: Sur les matériaux standard généralisés. Journal de mécanique **14**(1), 39–63 (1975)
7. Hecht, F.: New development in freefem++. J. Numer. Math. **20**(3-4), 251–265 (2012)
8. Klarbring, A., Barber, J., Spagnoli, A., Terzano, M.: Shakedown of discrete systems involving plasticity and friction. Eur. J. Mech. A **64**, 160–164 (2017)
9. Miehe, C.: Strain-driven homogenization of inelastic microstructures and composites based on an incremental variational formulation. International Journal for numerical methods in engineering **55**(11), 1285–1322 (2002)
10. Miehe, C., Lambrecht, M., Gürses, E.: Analysis of material instabilities in inelastic solids by incremental energy minimization and relaxation methods: evolving deformation microstructures in finite plasticity. Journal of the Mechanics and Physics of Solids **52**(12), 2725–2769 (2004)
11. Morel, F., Palin-Luc, T.: A non-local theory applied to high cycle multiaxial fatigue. Fatigue & Fracture of Engineering Materials & Structures **25**(7), 649–665 (2002)
12. Morel, F., Palin-Luc, T., Froustey, C.: Comparative study and link between mesoscopic and energetic approaches in high cycle multiaxial fatigue. International journal of fatigue **23**(4), 317–327 (2001)
13. Mróz, Z., Seweryn, A.: Damage description with related crack initiation and propagation conditions. Journal de Physique IV Proceedings **06**(C6), 529–538 (1996)
14. Mura, T.: Micromechanics of defects in solids. Springer Science & Business Media (1987)
15. Nguyen, P.H., Le, C.V., Ho, P.L.: Numerical evaluation of macroscopic fatigue criterion of anisotropic materials using computational homogenisation and conic programming. European Journal of Mechanics-A/Solids p. 104654 (2022)
16. Peigney, M., Seguin, J.: An incremental variational approach to coupled thermomechanical problems in anelastic solids. Application to shape-memory alloys. International Journal of Solids and Structures **50**(24), 4043–4054 (2013)
17. Peigney, M.: Shakedown theorems and asymptotic behaviour of solids in nonsmooth mechanics. Eur. J. Mech. A **29**, 784–793 (2010)
18. Peigney, M.: On shakedown of shape memory alloys structures. Ann. Solid Struct. Mech. **6**, 17–28 (2014)
19. Peigney, M.: Shakedown of elastic-perfectly plastic materials with temperature-dependent elastic moduli. J. Mech. Phys. Solids **71**, 112–131 (2014)
20. Peigney, M.: Cyclic steady states in diffusion-induced plasticity with applications to lithium-ion batteries. Journal of the Mechanics and Physics of Solids **111**, 530–556 (2018)
21. Peigney, M.: Static and kinematic shakedown theorems in diffusion-induced plasticity. Journal of Theoretical and Applied Mechanics **58** (2020)

22. Peigney, M., Scalet, G., Auricchio, F.: A time integration algorithm for a 3d constitutive model for smas including permanent inelasticity and degradation effects. International Journal for Numerical Methods in Engineering **115**(9), 1053–1082 (2018)
23. Peigney, M., Seguin, J., Hervé-Luanco, E.: Numerical simulation of shape memory alloys structures using interior-point methods. International journal of solids and structures **48**(20), 2791–2799 (2011)
24. Pham, D.C.: Consistent limited kinematic hardening plasticity theory and path-independent shakedown theorems. Int. J. Mech. Sci. **130**, 11–18 (2017)
25. Sakout, S., Weisz-Patrault, D., Ehrlacher, A.: Energetic upscaling strategy for grain growth. I: Fast mesoscopic model based on dissipation. Acta Materialia **196**, 261–279 (2020)
26. Scalet, G., Peigney, M.: A robust and efficient radial return algorithm based on incremental energy minimization for the 3D Souza-Auricchio model for shape memory alloys. European Journal of Mechanics - A/Solids **61**, 364–382 (2017)
27. Vandenberghe, L., Mutapcic, A.: Maximum volume inscribed ellipsoid in a polyhedron. Boyd and Vandenberghe "Convex Optimization" (Jan 2006)